Desalination and Water Treatment
www.deswater.com
doi: 10.1080/19443994.2015.1026278

57 (2016) 8776–8788
April

Taylor & Francis
Taylor & Francis Group

Ultrasound-assisted synthesis and characterization of visible light responsive nitrogen-doped TiO_2 nanomaterials for removal of 2-Chlorophenol

Nidhi Sharotri, Dhiraj Sud*

Department of Chemistry, Sant Longowal Institute of Engineering and Technology (Deemed University), Longowal 148106, Sangrur, Punjab, India, Tel. +919478074338; Fax: +911672280057; email: nidhisliet11@gmail.com (N. Sharotri), Tel. +919463067540; Fax: +911672280057; email: suddhiraj@yahoo.com (D. Sud)

Received 27 May 2014; Accepted 28 February 2015

ABSTRACT

Ultrasound-assisted synthesis of nanosized N-doped TiO_2 was carried out by using titanium isopropoxide as titanium precursor and hydroxylamine hydrochloride as an inorganic template. The synthesized nano-plaits have been characterized using X-ray diffraction, scanning electron microscopy, energy dispersive X-ray spectroscopy, transmission electron microscopy, Brunauer–Emmett–Teller surface area, Fourier transform infrared spectrometer, ultraviolet–visible absorption (UV–vis), and Raman spectroscopy. The influence of reaction parameters (solvent, reaction time, and calcination temperature) on particle size and surface morphology has also been investigated. The morphological studies confirm the successful synthesis of anatase TiO_2 nano-plaits having a particle size of 10 nm and shows absorption (576 nm) in a visible region. The effect of calcination on crystalline size of the TiO_2 was investigated by varying the calcination temperature. The photocatalytic activity of the synthesized catalyst was investigated for the degradation of 2-Chlorophenol under various wavelengths of visible light (490, 565, and 660 nm). N-doped TiO_2 nano-plaits exhibited promising photocatalytic activity and 79.8% of 2-Chlorophenol is degraded in the visible region of wavelength 660 nm at pH 8.

Keywords: Ultrasound; Photocatalysis; N-doped Titania; Spectroscopic techniques; Degradation; 2-Chlorophenol

1. Introduction

Heterogeneous photocatalysis using semiconductors has emerged as a potent destructive technology for phasing out the organic pollutants from environmental matrix [1,2]. Semiconductors such as CdS, SnO_2, WO_3, TiO_2, $ZrTiO_4$, and ZnO are considered as photocatalysts because of their ability to absorb light [3]. Titanium dioxide (TiO_2) is extensively applied to air and water purification, water disinfection, and antibacterial protection [4]. TiO_2 is a preferred photocatalyst because of its biological and chemical inertness, nontoxicity, and strong oxidizing power [5,6]. Still, the commercial and industrial applications of the process have been foiled because of the inability of TiO_2 to exploit the vast potential of solar radiations.

The wide band gap of TiO_2 (3.2 eV) [7], which corresponds to wavelengths shorter than 387 nm, results in its excitation by UV light photons (< 380 nm) and can capture only less than 10% of the solar radiation. Hence, the impetus of the research lies

*Corresponding author.

in the development of visible light-responsive TiO_2 materials for degradation of environmental pollutants. This can be achieved by (i) semiconductor coupling, (ii) surface modification, (iii) band gap modification by creating oxygen vacancies, and (iv) metals and non-metals doping [8–10]. Doping is the addition of controlled amounts of specific impurity atoms for the purpose of narrowing the band gap. Attempts have been taken for doping of p-block elements (C, N, F, P, or S) to replace O in the anatase phase of TiO_2. Among these, N-doping has been considered as an efficient mode for the production of visible light-responsive photocatalyst. The absorption of visible light may result in a narrowing of the band gap of the N-doped TiO_2 formed by substitution of O atoms by a nitrogen atom in Titania lattice or oxygen vacancies created by N doping or mixing of N (2p) states with O (2p) states [11,12].

Different techniques used to dope nitrogen into TiO_2 lattice include a hydrothermal method [13], hydrolysis of organic and inorganic titanium compounds in ammonia water, followed by heating the resultant precipitates or their mixtures with urea [14], the mechanochemical reaction of titanium with urea [15], spray pyrolysis [16], and oxidation of titanium nitride [17]. Xing et al. [18] successfully synthesized and characterized nitrogen-doped TiO_2 photocatalyst with higher visible light activity for the degradation of 2,4-dichlorophenol. Sun et al. [19] investigated the degradation efficiency of nitrogen-doped TiO_2 catalyst under visible light and sunlight using Orange G as a pollutant. Sin et al. [20] reported the effect of UV irradiation in the presence of nanophotocatalyst (TiO_2, ZnO) for the degradation of two selected endocrine-disputing chemicals like phenols and resorcinol. The mechanism for the degradation of resorcinol by TiO_2 and ZnO nanophotocatalyst has been proposed by Lam et al. [21].

The catalytic behavior depends upon the size and characteristics of nanomaterials and shows the variation in optical and electronic properties with size. Ultrasound-assisted nanomaterials synthesis is emerging as an important tool for synthesis of metal oxide nanoparticles with controlled morphology. The physical and chemical effect generated by acoustic cavitations during ultrasonication significantly influences the size and properties of nanoparticles [22]. The literature survey reveals that synthesis of N-doped TiO_2 using sonochemical method has not been reported except its use as pre-treatment *in situ* pyrolysis for preparation of mesoporous TiO_2−xNx [23].

Chlorophenols are known organic pollutants found in wastewater released from industries, such as petroleum refining, steel, dyestuff, synthetic resins, byproducts of agricultural chemicals, paper and pulp mills, tanning, and fiberboard product, into the environment. It is also an essential chemical feedstock in the manufacturing of higher chlorophenols, which are used as fungicides, bactericides, antiseptics, disinfectants, and wood and glue preservatives. Therefore, 2-Chlorophenol was selected as model compound for studying the photocatalytic activity of synthesized N-doped TiO_2 catalyst.

N-doped TiO_2 photocatalyst was synthesized using an inorganic template under ultrasonic irradiation at 40 kHz. The effect of calcination temperature and reaction conditions, i.e. solvent and time of ultrasonication on structural morphology of catalyst was investigated. The photocatalytic activity of the N-doped TiO_2 has been measured for the photocatalytic degradation of 2-Chlorophenol using different regions of the solar spectrum.

2. Experimental

2.1. Chemicals

Titanium isopropoxide (98%) was purchased from Sigma-Aldrich. Hydroxylamine hydrochloride used as a nitrogen precursor was acquired from Himedia. Solvents like methanol, ethanol, isopropyl alcohol, and butanol used were of analytical grade. 2-Chlorophenol was purchased from SD Fine-Chem. Limited.

2.2. Synthesis of N-doped TiO_2 photocatalyst

Titanium isopropoxide (8.52 g) was dissolved in 20 ml ethanol and ethanolic solution of hydroxylamine hydrochloride (2.085 g) was added dropwise with constant stirring. The resultant solution was further stirred for half an hour followed by the addition of NH_4OH solution. Thereafter, the resultant mixture was put under ultrasonic bath and was exposed to sound waves of 40 kHz for 40 min, then the solution was kept overnight. The precipitates formed were filtered by vacuum filtration, crystallized with methanol, and dried in oven at 100˚C for 2 h. The synthesized nitrogen-doped TiO_2 precipitates were yellowish in colour and calcinated at different temperatures (350, 450, 550, and 750˚C). The effect of solvent on the morphological properties of the synthesized photocatalyst was studied by carrying the reaction in different solvents viz. methanol, isopropyl alcohol, and butanol and the products were calcinated at 450˚C. The reaction conditions were further optimized by varying the ultrasonication time (10–60 min).

2.3. Characterization of N-doped TiO_2 nanoparticles

The phase and structure identification of the as-synthesized nitrogen-doped TiO_2 was performed by X-ray diffraction (XRD) technique. X-ray diffractometer (XPERT-PRO) employing Cu *K*_radiation (= 0.15406 nm) with a scanning rate of 5°/min in the 2θ angle ranged from 20 to 80° was used. The IR spectra were recorded on an FTIR spectrometer (Spectrum One, PerkinElmer). The UV–vis absorption spectra of the samples were recorded using UV–vis spectrophotometer (UV-1800, Shimadzu). The morphology and size of TiO_2 nano-plaits were measured by MORGAGNI-268E transmission electron microscopy (TEM) and JSM-6,610-JEOL/EO scanning electron microscopy (SEM) at an accelerating voltage of 15 kV. Raman spectra were recorded with (Make-JY -HORIBA) Model-iHR Spectrograph. The specific surface area was determined by N_2 adsorption method using smartsorb 91/92 instrument after preheating 100 mg samples at 150°C for 1 h. The samples were regenerated at 175°C for 90 min.

2.4. Experimental setup and procedure for photocatalytic degradation

Photocatalytic degradation was carried out in specially designed double-walled reaction vessels (volume 250 ml) in the photocatalytic chamber equipped with LED bulbs of different wavelengths (490, 565, and 660 nm). Constant stirring of the solution was provided using magnetic stirrers and the aeration was done using aerators. The photocatalytic activity of as-synthesized N-doped TiO_2 has been investigated by irradiation of 50 ml suspension of 2-Chlorophenol (25 ppm) and N-doped TiO_2 (50 mg) under visible light. At different time intervals, an aliquot was taken out with the help of syringe and then filtered through Millipore syringe filter of 0.22 μm. The rate of degradation of 2-Chlorophenol was studied spectrophotometrically by studying the changes in absorption spectra recorded for the samples at 273 nm. The degradation efficiency (%) has been calculated as follows:

$$\text{Efficiency } (\%) = (C_0 - C)/C_0 \times 100 \quad (1)$$

3. Result and discussion

Ultrasound-assisted synthesis of photocatalyst N-doped TiO_2 was carried out using titanium isopropoxide and hydroxylamine hydrochloride.

The resultant amorphous product was calcinated at different temperatures (350, 450, 550, and 750°C). Further, the effect of varying the reaction conditions such as reaction time and solvent has also been studied. The synthesized calcinated products were characterized by employing different techniques.

3.1. XRD analysis of NT-450

The XRD analysis of synthesized TiO_2 and N-doped TiO_2 calcinated at 450°C (NT-450) was carried out to investigate the crystal structure. The typical XRD patterns of the synthesized undoped TiO_2 and NT-450 shows strong diffraction peaks at 25.4, 37.05, 38.6, 48.15, 53.92, and 75.28° (Fig. 1). The observed patterns were matched with JCPDS card number 01-073-1764, which reflects the formation of anatase phase as the main crystal phase.

3.1.1. Effect of calcination temperature on the crystalline phase

The synthesized catalyst N-doped TiO_2 was calcinated at various temperatures; 350, 450, 550, 650, and 750°C in order to study the effect of calcination temperature on the crystalline phase shown in Fig. 2. The XRD pattern for the samples calcinated at 350, 450, 550, and 650°C shows only anatase phase. However, at 750°C, it was observed that the phase transformation occurs and peaks in both the anatase and rutile phases. The sample shows peaks at 25.4, 37.05, 38.6, 48.15, 53.92 and 27.49°, 36.1, 39.22, 41.26, 44.07, 53.87, 56.70, 62.63, 69.08, 72.61, and 76.61°, respectively, for anatase and rutile at 750°C.

The percentage of the respective peaks corresponding to different phase has been calculated by applying equation [24].

$$\text{Fraction of rutile phase} = {}^{1}/_{1 + 0.79(I_A/I_R)} \quad (2)$$

where I_A is the intensity of the anatase phase and I_R is that of the rutile phase. At 750°C, 59% of the anatase phase and 41% of the rutile phase appears. It can be seen that the N-doped TiO_2 samples show peak broadening as compared to the undoped TiO_2 and is in agreement with the earlier reported results [25]. The average crystallite size of the synthesized N-doped TiO_2 has been calculated by applying Scherrer equation [26].

$$D = K\lambda/\beta\cos\theta \quad (3)$$

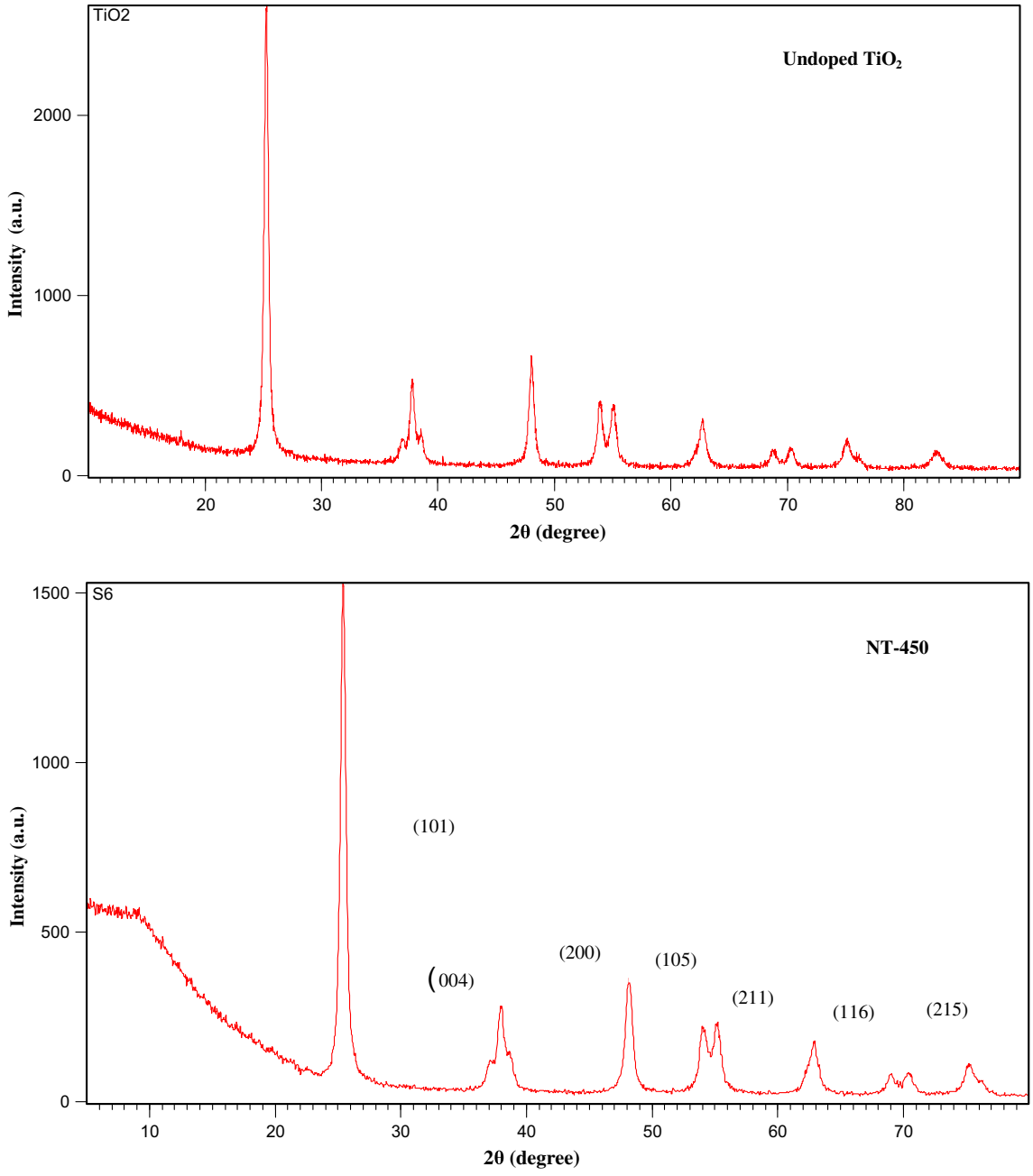

Fig. 1. XRD Pattern of NT-450.

where λ is the wavelength of the X-ray employed, β is the full width at half maximum in the radiation of the peak, θ the Bragg's angle of the XRD peak, and K the Scherrer shape factor, $K = 0.9$. The average crystallite size of the samples is found to be 23.1, 25.71, 28.5, 30.6, 33.06, and 46.2 nm, respectively, for undoped TiO_2 and N-doped TiO_2 (calcinated at 350, 450, 550, 650, and 750°C). The lattice parameters for synthesized NT are calculated by applying d-spacing formulae.

$$1/d^2hkl = h^2k^2l^2/a^2b^2c^2 \quad (4)$$

where d is the interplanar distance, hkl are the Miller indices and a, b, and c are the side lengths of the tetragonal crystal system. The results confirmed that the pattern had tetragonal crystal structure and anatase phase (Table 1).

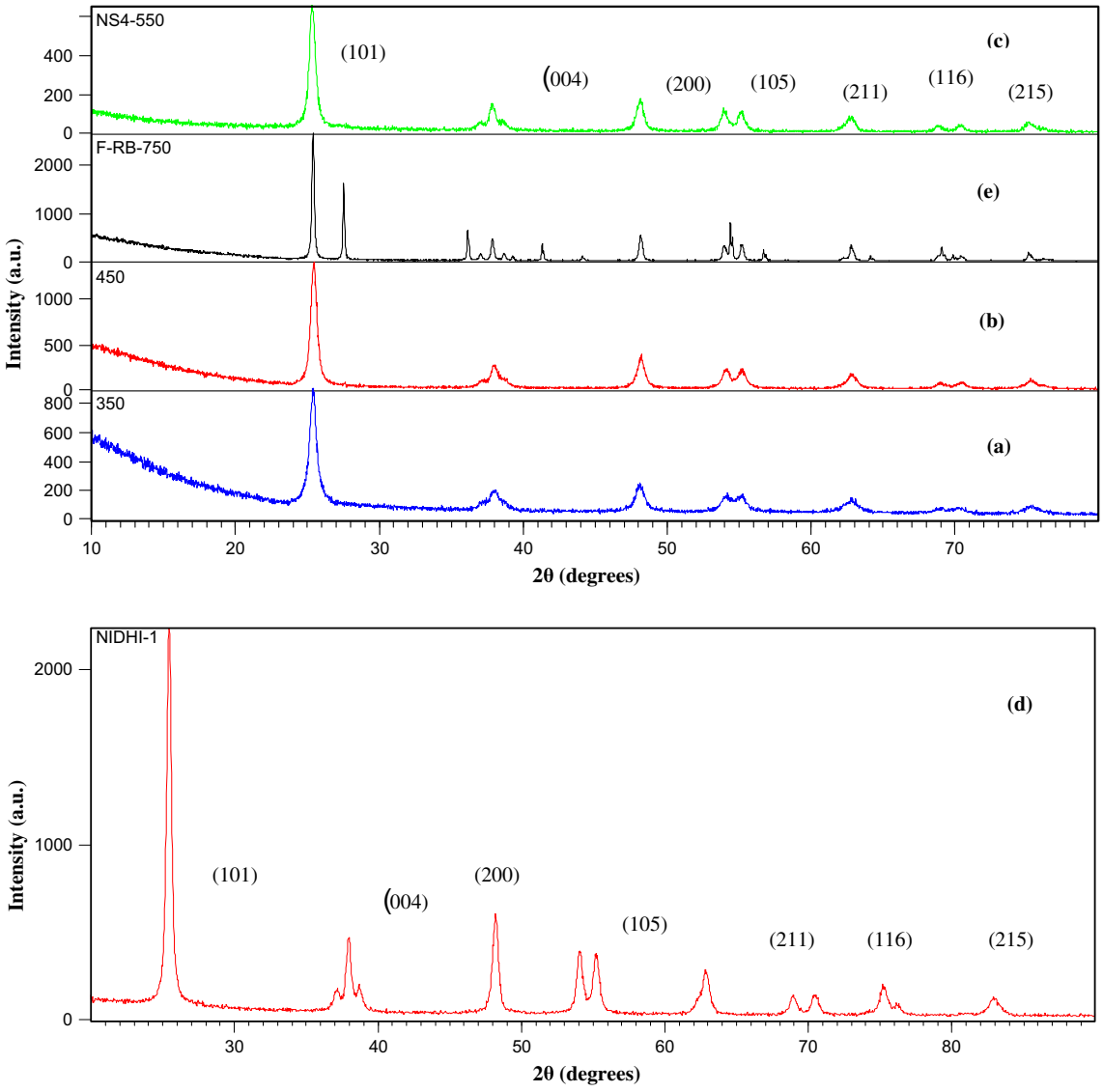

Fig. 2. XRD patterns of N-doped TiO_2 calcinated at different calcination temperatures: (a) 350˚C, (b) 450˚C, (c) 550˚C, (d) 650˚C, and (e) 750˚C.

Table 1
The crystal phase, interplanar distance, and *d*-spacing value of N-doped TiO_2 calcinated at different temperatures

S. No.	Calcination treatment (˚C)	Lattice parameters		*d*-spacing (A˚)	Crystalline phase
		a	*b*		
1.	Pure TiO_2	3.776	9.486	3.54	Anatase
2.	350	3.765	9.454	3.50670	Anatase
3.	450	3.765	9.454	3.50725	Anatase
4.	550	3.765	9.454	3.50661	Anatase
5.	650	3.765	9.454	3.50661	Anatase
6.	750	3.765	9.454	3.50730	Rutile + Anatase

3.2. Morphological studies and elemental composition of NT-450

3.2.1. SEM and EDX

The surface morphology and elemental composition of the NT-450 nanoparticle have been investigated by SEM and EDX micrographs, respectively, shown in Figs. 3(b) and 4. Morphological studies of as-synthesized NT-450 nanoparticles show the formation of clusters of fibrous structures entangled to give a flowery appearance. The elemental composition of the NT-450 as determined by chemical microanalysis technique EDX confirms the nitrogen doping into the TiO_2 lattice, i.e. 7.49 at.% nitrogen incorporated into TiO_2 lattice.

3.2.1.1. Effect of calcination temperature on surface morphology. The effect of calcination temperature (i.e. at 350, 450, 550, and 750˚C) on the surface morphology of synthesized photocatalyst has been investigated. SEM image (Fig. 3) shows the growth in particle size with an increase in calcination temperature and at the 750˚C, change in appearance was observed. The change may be due to occurrence of phase transformation at 750˚C as confirmed by XRD pattern.

3.2.1.2. Effect of solvent on surface morphology. The different solvents such as methanol, ethanol, isopropyl alcohol, and butanol employed for the synthesis of N–TiO_2 and their effect on surface morphology was

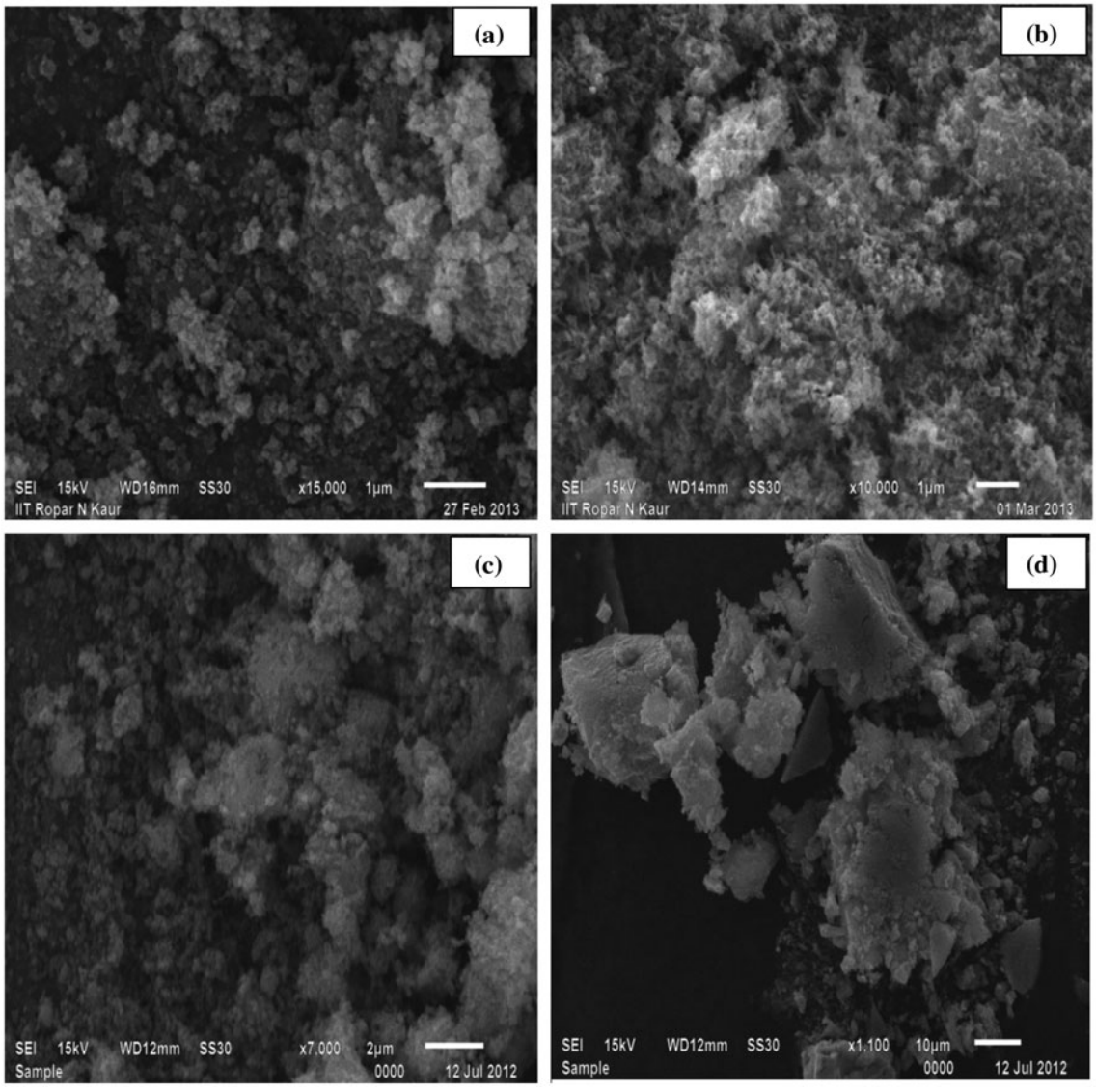

Fig. 3. SEM image showing effect of variation of calcination temperature: (a) 350˚C, (b) 450˚C, (c) 550˚C, and (d) 750˚C.

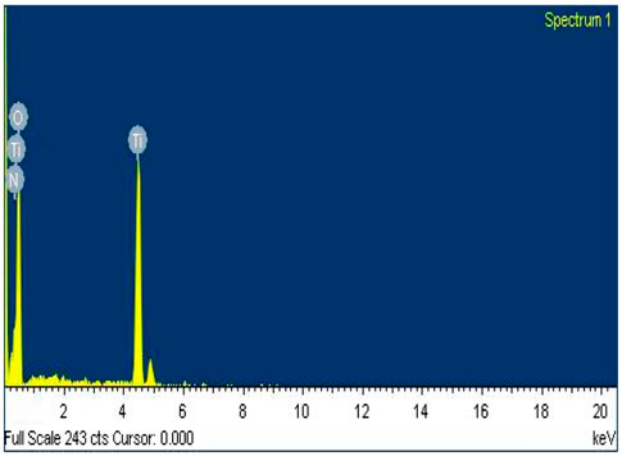

Fig. 4. EDX spectra of NT-450.

examined (Fig. 5). The study shows that solvents have a noticeable effect on the size and morphology of nanoparticles formed and larger particle size was observed for higher molecular weight solvents. The particle size increase in the order: methanol<ethanol<isopropyl alcohol<n-butanol. Such a trend may be attributed to the fact that ultrasonication is related to cavitations. Cavitations cause the solute thermolysis along with the formation of highly reactive radical and reagents. Both high solvent viscosity and high surface tension inhibit cavitations because of the higher natural cohesive forces acting within the liquid. A change in the surface morphology was found with isopropyl alcohol and butanol, and the catalysts with rocky appearance are formed [24].

3.2.1.3. Effect of ultrasonication time. The effect of ultrasonication time on percentage yield was studied by irradiation of the sample with sound waves of 40 kHz for different time intervals, i.e. at 10, 20, 40, and 60 min, respectively. The maximum yield of the NT-450 was obtained for sample irradiated for 40 min. The EDX spectrum shows that as the sound wave irradiation time increases, the incorporation of nitrogen also increases. This results in 1.41, 2.44, 7.49, and 9.33 at.% of the nitrogen being incorporated, respectively (Fig. 6). Thus, optimum conditions for the synthesis of the NT were found to be an ultrasonication time of 40 min in the presence of ethanol and calcinated at 450°C.

3.2.2. Transmission electron microscopy

A deep insight into the nanostructure of NT-450 photocatalyst has been obtained from TEM observation. The TEM image shown in Fig. 7 confirms the formation of nanorange (10–100 nm) photocatalyst and the observed pattern shows the formation of entangled plaits having the particle size of approximately 10 nm. The surface area analysis confirms that the surface area of NT-450 was 85 m^2/g.

3.3. Spectroscopic studies of NT-450

3.3.1. FT-IR spectrum

Fourier transform infrared spectrometer (FT-IR) spectrum of NT-450 sample is shown in Fig. 8. A strong band at 2,500–3,700 cm^{-1} and narrow band at 1,628 cm^{-1} was assigned to the hydroxyl group stretching and bending vibrations. The IR peaks observed in 1,384, 1,163, and 1,019 cm^{-1} confirmed the substitution of nitrogen atoms into TiO_2 network and is in agreement with earlier reported results. IR spectral peaks corresponding to the N–H modes imply the successful doping of nitrogen atoms. Low-frequency bands observed at 400–900 cm^{-1} corresponds to vibration mode of anatase skeletal O–Ti–O bond with a maximum of 465 cm^{-1} [6,27].

3.3.2. Raman spectra

The Raman spectrum shows the main peak at 143 cm^{-1} and smaller peaks at 397, 519, and 638 cm^{-1} (Fig. 9), which supports that the anatase is a predominant phase structure [26].

3.3.3. UV–vis absorption spectra

Fig. 10 depicts the UV–vis spectra and band gap study of the NT-450. The absorption spectrum of NT-450 shows absorption at 576 nm, which ensures a significant shift towards the visible region due to the introduction of a small amount of nitrogen. The band gap energy of the NT-450 sample was calculated using equation [23].

$$E\ (eV) = \mathrm{hc}/\lambda = 1,239.95/\lambda \quad (5)$$

where E is the band gap energy (eV), h is Planck's constant, c is the velocity of light (m/s), and λ is the wavelength in nm.

Table 2 compiles the band gaps reported by researchers for the N-doped TiO_2 synthesized using different techniques [23,26,28,29]. The as-synthesized NT-450 shows absorption at 576 nm, with a band gap of 2.15 eV. The narrowing of the band gap has been

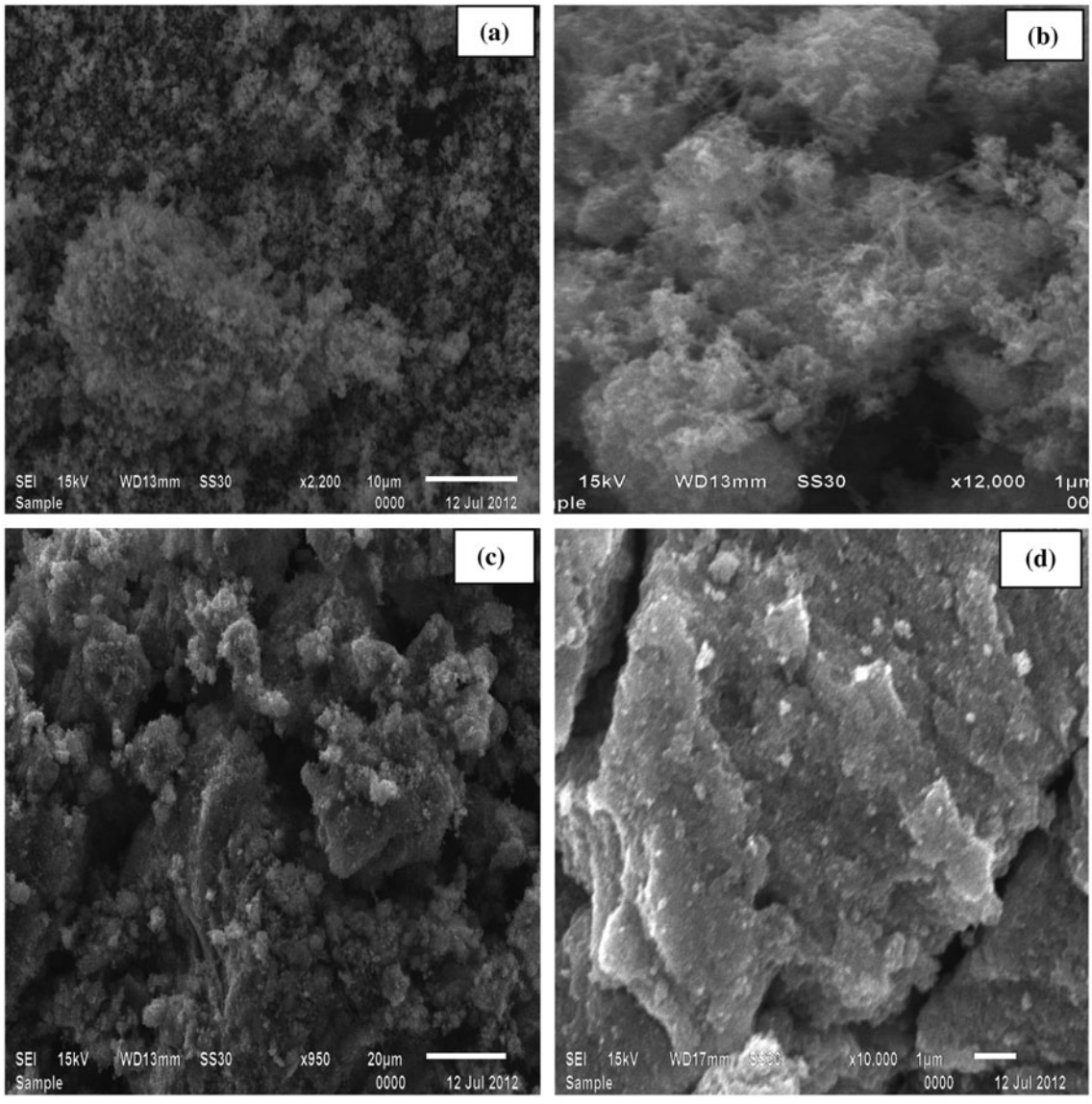

Fig. 5. Effect of solvent on surface morphology of NT-450: (a) Methanol, (b) Ethanol, (c) Isopropyl alcohol, and (d) Butanol.

described on the basis of mixing of the N_{2P} and the O_{2P} states [23] because the nitrogen ions substitute for the oxygen in the TiO_2 lattice. In general, the absorption edge of TiO_2 around 400 nm was ascribed to the band transition from O 2p to Ti 3d. When the small amount of nitrogen replaces oxygen, the hybridization is held between O 2p and N 2p. The energy of the hybridized 2p is higher than that of the pure O 2p orbital [29].

3.4. Photocatalytic activity of synthesized NT-450

2-Chlorophenol shows an absorption peak at 273 nm in UV region. The degradation percentage was recorded with respect to the change in intensity of absorption peak at 273 nm.

The photocatalytic activity of synthesized N-doped TiO_2 nanophotocatalyst calcinated at different temperatures viz. 350, 450, 550, and 750˚C was studied using 2-Chlorophenol. The Fig. 11 shows 43.5, 79.8, 60.2, and 39.7% degradation using NT-350, NT-450, NT-550, and NT-750. The maximum photocatalytic activity was shown by NT-450, thus it was selected for degradation of 2-Chlorophenol.

The response of NT-450 towards the degradation efficiency of 2-Chlorophenol was investigated in various wavelength regions of the solar spectrum (490, 565, and 660 nm). Fig. 12 shows that the percentage

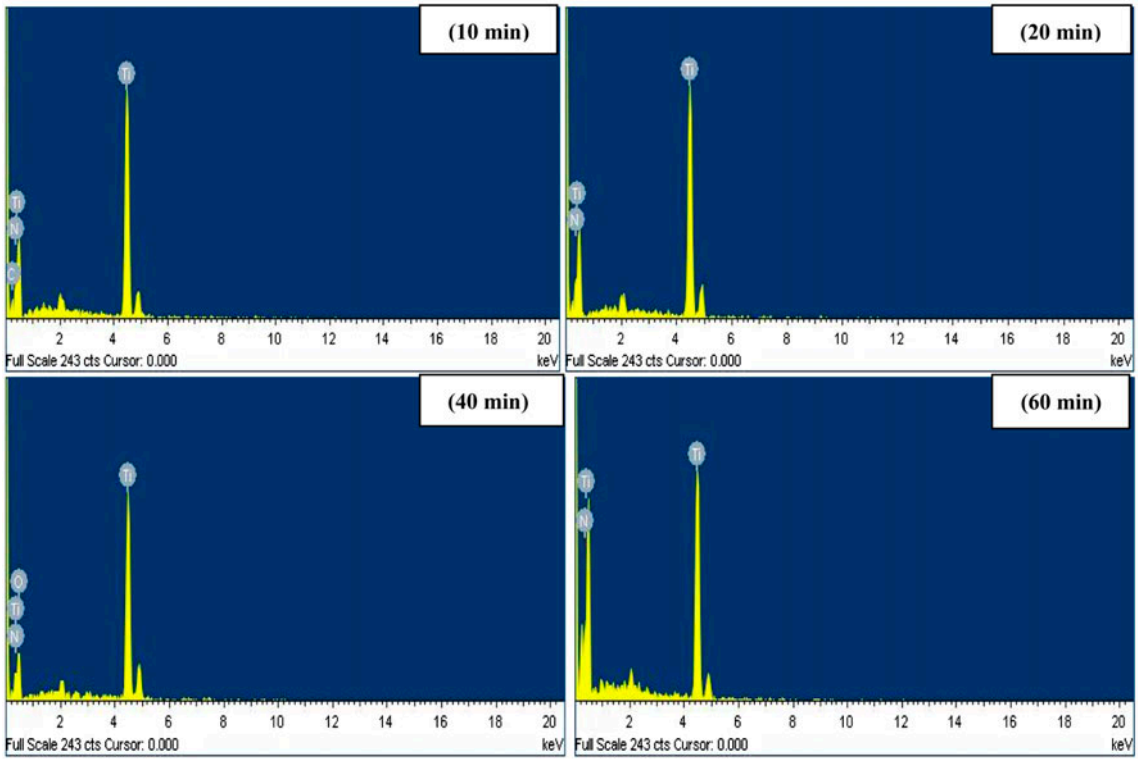

Fig. 6. EDX micrograph of NT-450 ultrasonicated for different time intervals (10, 20, 40, and 60 min).

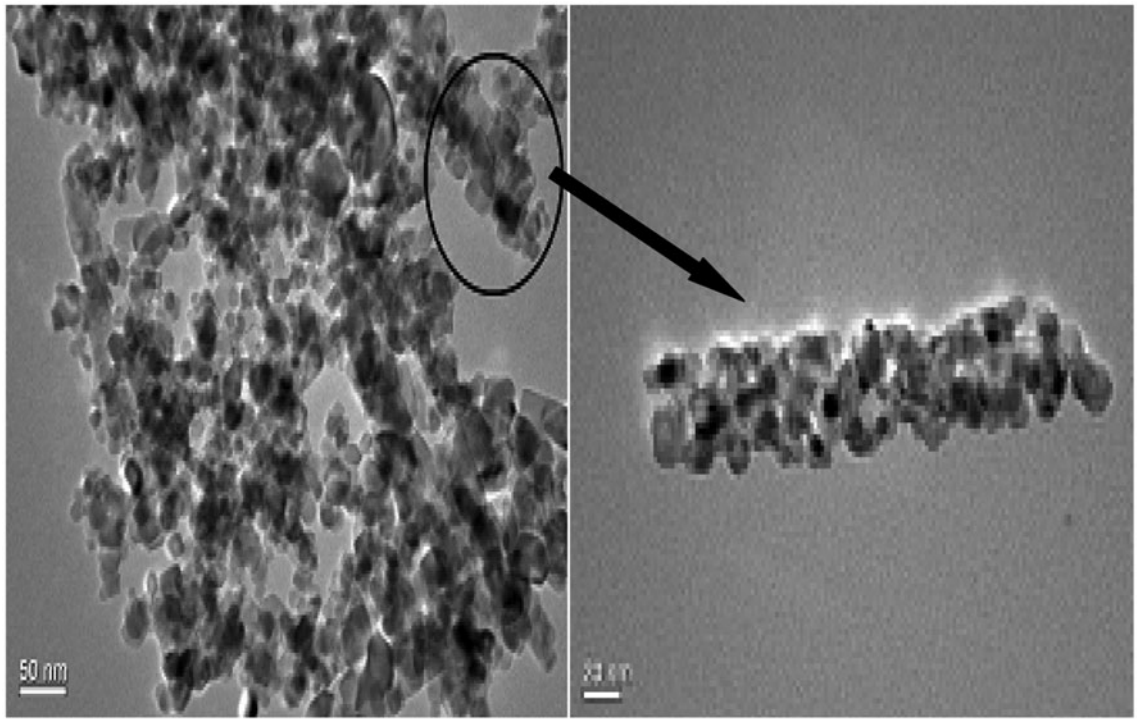

Fig. 7. TEM image of NT-450.

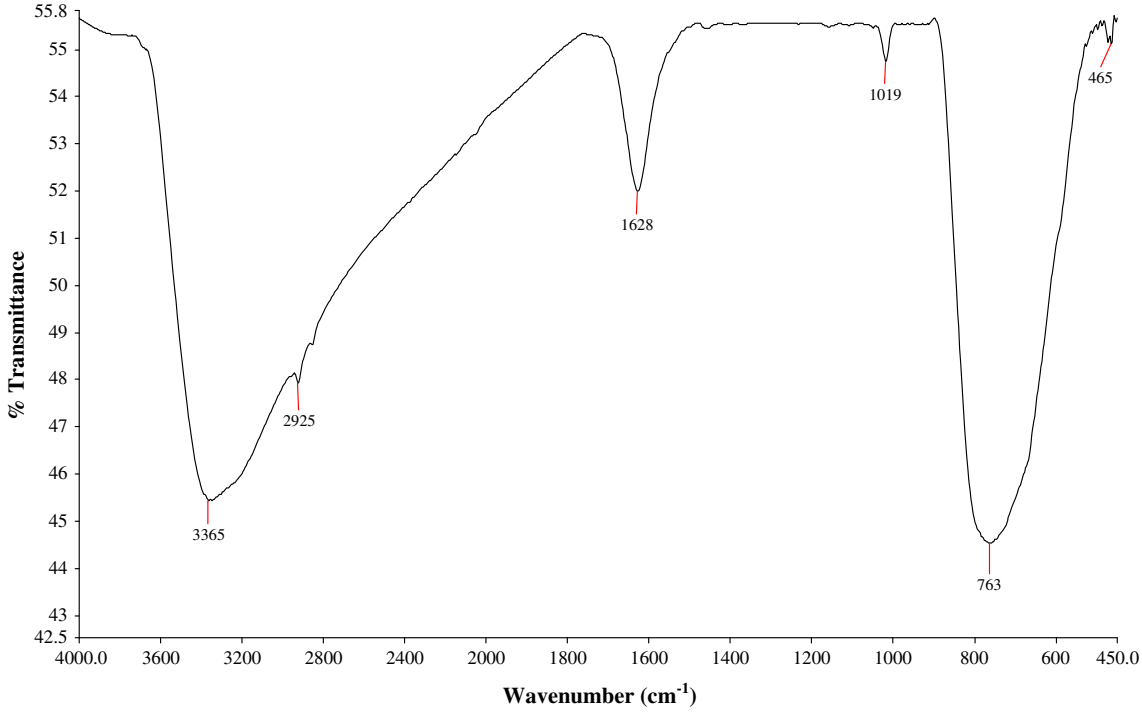

Fig. 8. FT-IR Spectrum of the synthesized NT-450.

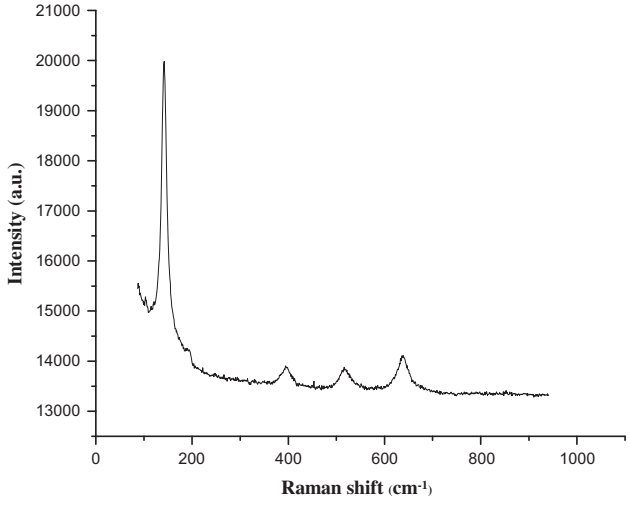

Fig. 9. Raman spectra of synthesized NT-450.

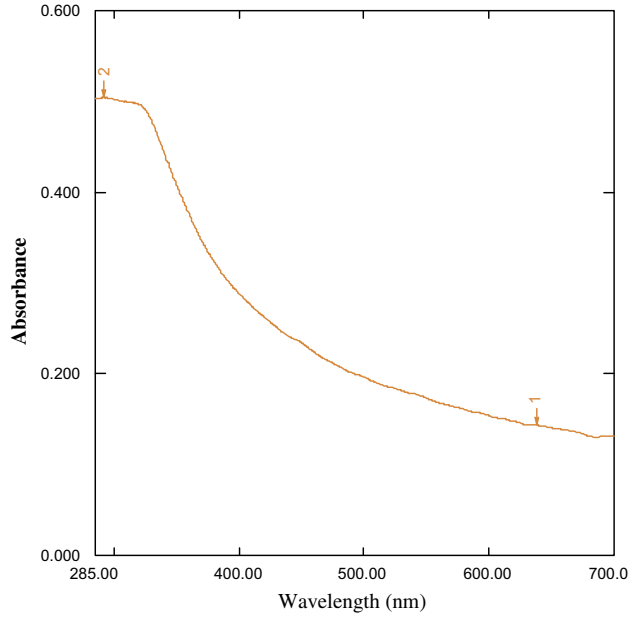

Fig. 10. UV–vis Spectra of synthesized NT-450.

degradation at different wavelengths 660, 565, and 490 nm was 79.8, 57.7, and 70%, respectively. The maximum degradation efficiency (% degradation) was observed at 660 nm. Therefore, a red region (660 nm) having a light intensity of about 100 μmol $m^{-2}s^{-1}$ was chosen for further investigations.

Photocatalytic degradation of 2-Chlorophenol has been studied under four different conditions: (i) Red light (660 nm), (ii) undoped TiO_2 under dark, (iii) doped NT-450 under dark, and (iv) doped NT-450 under red light. Fig. 13 confirms that 79.8% of the 2-Chlorophenol was degraded in the presence of NT-450 under exposure to the red region of light.

Table 2
Comparative studies of band gap in literature

S. No.	λ_{max} (nm)	Band gap (eV)	References
1	440	2.81	[24]
2	447	2.72	[26]
3	451	2.70	[26]
4	470	2.64	[28]
5	483	2.56	[28]
6	600	2.07	[29]

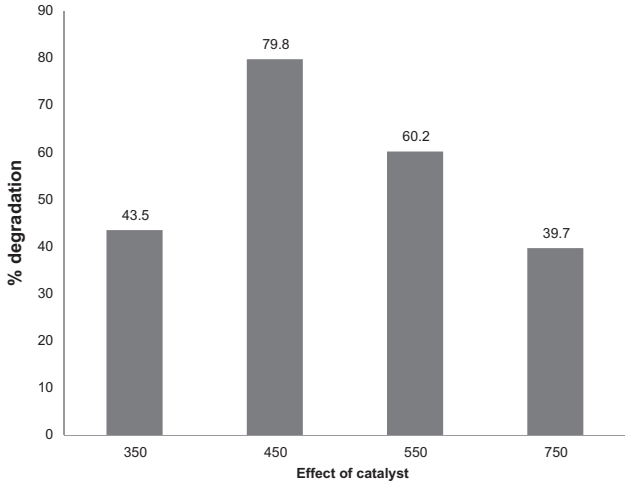

Fig. 11. Effect of calcination temperatures (350, 450, 550, and 750) on the percentage degradation of 2-Chlorophenol.

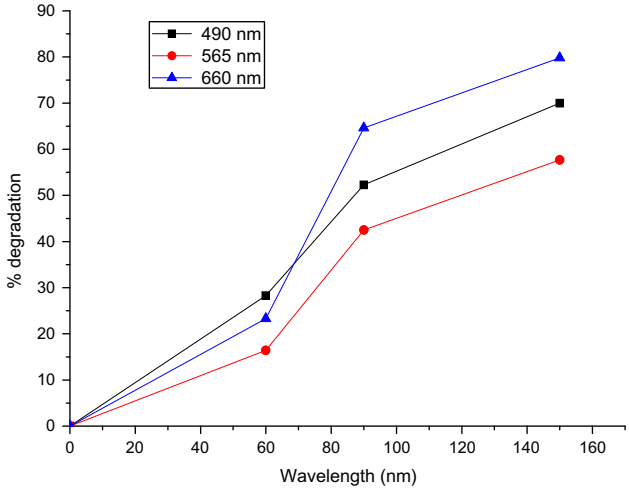

Fig. 12. Effect of various wavelength regions (490, 565, and 660 nm) on the percentage degradation of 2-Chlorophenol (concentration = 25 ppm, catalyst dose = 50 mg/50 mL, and pH 8).

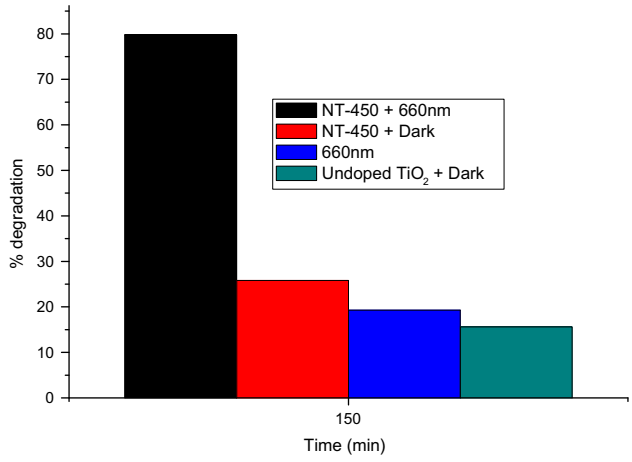

Fig. 13. Photocatalytic degradation of 2-Chlorophenol under four different conditions: (i) 660 nm, (ii) Dark + undoped TiO_2, (iii) Dark + NT-450, and (iv) 660 nm + NT-450.

Time-dependent UV–vis spectra (Fig. 14) shows the photocatalytic degradation of 2-Chlorophenol with NT-450 at 660 nm. The absorption peak diminished gradually and 79.8% of the 2-Chlorophenol has been degraded within 150 min. Nitrogen-doped TiO_2 nanophotocatalyst (NT-450) shows absorption in the visible region with maximum efficiency in red region. Nitrogen doping decreases the band gap and helps in transferring of electron from N2p to conduction band of TiO_2. The mechanism of the process was summarized below.

First step is the generation of electron/hole pair by absorption of solar light. The photogenerated electron/hole pair migrates to the surface of catalyst and forms active species, such as hydroxyl radical and superoxide ion [30]. These active species may participate in the photodecomposition of 2-Chlorophenol.

$$N\text{-}TiO_2 + hv \longrightarrow e^-_{(CB)}TiO_2 + h^+_{(VB)}TiO_2 \quad (6)$$

$$O_2 + e^-_{(CB)} \longrightarrow O^{\bullet -}_2 \quad (7)$$

$$O^{\bullet -}_2 + H_2O \longrightarrow {}^{\bullet}OH + OH^- \quad (8)$$

$$h^+_{(VB)} + OH^- \longrightarrow {}^{\bullet}OH \quad (9)$$

$${}^{\bullet}OH + C_6H_5ClO \longrightarrow \text{Intermediate} \longrightarrow CO_2 + H_2O \quad (10)$$

The pH of the solution plays a key role in the photocatalytic degradation of organic pollutants. Experiments were performed at various pH values

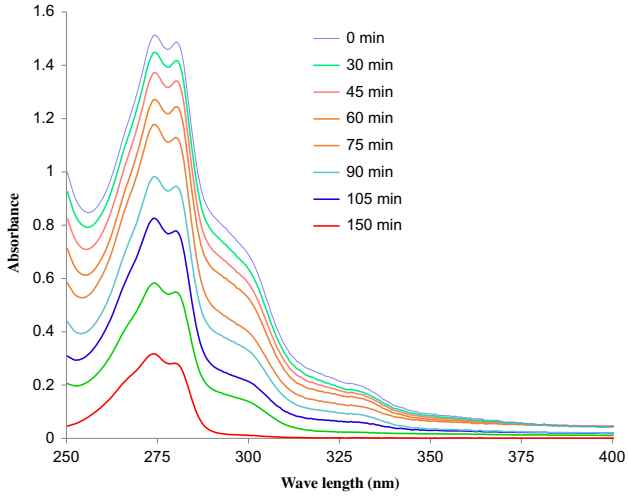

Fig. 14. Time-dependent UV–vis spectra of 2-Chlorophenol.

Table 3
Effect of pH on photocatalytic degradation of 2-CP

Parameters	Range	Percentage degradation (%)
pH	2	50.7
	4	53.3
	6	68.1
	8	79.8
	10	64.6

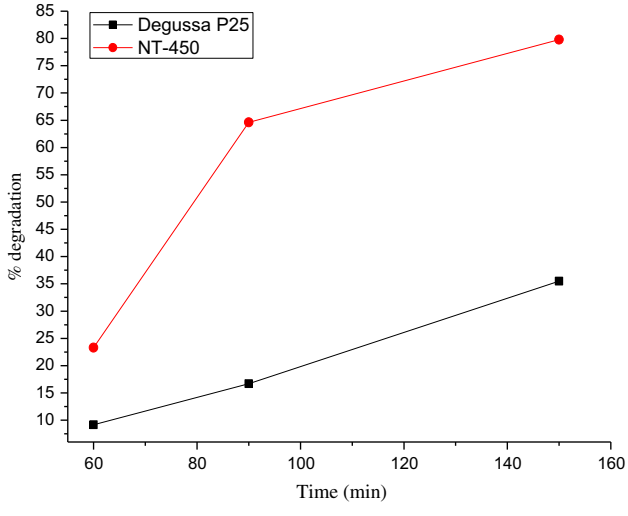

Fig. 15. Comparison of degradation efficiency of Degussa P25 and synthesized NT-450 (concentration = 25 ppm, catalyst dose = 50 mg/50 mL, and pH 8).

from 2 to 10. Maximum degradation was obtained at pH 8 for the constant pollutant (2-Chlorophenol) concentration (25 mg/L) and catalyst loading (50 mg). Higher percentage degradation was observed at pH 8 (79.8%) followed by 68.1, 64.6, 53.3, and 50.7% at pHs 6, 10, 4, and 2, respectively, shown in Table 3.

The comparison of degradation efficiency of N-doped TiO_2 and Degussa P25 reflects promising results in visible light of wavelength 660 nm. N-doped TiO_2 shows promising degradation efficiency (79.8%), whereas 35.6% of 2-Chlorophenol was degraded with Degussa P25 (Fig. 15). The degradation process is initiated by the photoexcitation of the catalyst. Thus, the doping of TiO_2 with nitrogen results in higher absorption, which results in better performance of the catalyst. N-doped TiO_2 photocatalyst shows maximum % degradation efficiency of 79.8% at 660 nm at pH 8.

4. Conclusion

The study reports the greener synthesis of anatase N-doped TiO_2 nanoparticles using ultrasound irradiation. SEM and TEM results showed the formation of entangled nano-plaits, having the particle size of approximately 10 nm. The nano-plaits corresponding to anatase phase of TiO_2 and the absorption spectra of the N-doped TiO_2 exhibited new absorption peak in the visible light region. The investigation on the photocatalytic activity of the N-doped TiO_2 nano-plaits shows promising results. Ultrasound-assisted synthesis of nanophotocatalyst can be employed as a greener technique for the synthesis of nanomaterials with diverse structural morphology having improved optical and electronic properties.

Acknowledgements

The author is grateful to Sant Longowal Institute of Engineering and Technology, Longowal, for providing various facilities and financial support. The authors are pleased to acknowledge the facilities provided from Indian Institute of Technology, Ropar; Panjab University, Chandigarh; All India Institute of Medical Sciences (AIIMS), Delhi.

References

[1] M.A. Fox, M.T. Dulay, Heterogeneous photocatalysis, Chem. Rev. 93 (1993) 341–357.
[2] S. Lathasree, A.N. Rao, B. SivaSankar, V. Sadasivam, K. Rengaraj, Heterogeneous photocatalytic mineralisation of phenols in aqueous solutions, J. Mol. Catal. A: Chem. 223 (2004) 101–105.

[3] C.L. Wong, Y.N. Tan, A.R. Mohamed, A review on the formation of titania nanotube photocatalysts by hydrothermal treatment, J. Environ. Manage. 92 (2011) 1669–1680.
[4] J. Yu, G. Wang, B. Cheng, M. Zhou, Effect of hydrothermal temperature and time on the photocatalytic activity and microstructures of bimodal mesoporous TiO_2 powders, Appl. Catal., B 69 (2007) 171–180.
[5] J. Zhang, X. Xiao, J. Nan, Hydrothermal-hydrolysis synthesis and photo catalytic properties of nano-TiO_2 with an adjustable crystalline structure, J. Hazard. Mater. 176 (2010) 617–622.
[6] Y. Li, Y. Jiang, S. Peng, F. Jiang, Nitrogen doped TiO_2 modified with NH_4F for efficient photo catalytic degradation of formaldehyde under blue light-emitting diode, J. Hazard. Mater. 182 (2010) 90–96.
[7] M. Miyauchi, A. Nakajima, T. Watanabe, K. Hashimoto, Photocatalysis and photoinduced hydrophilicity of various metal oxide thin films, Chem. Mater. 14 (2002) 2812–2816.
[8] L. Wu, J.C. Yu, X. Fu, Characterization and photocatalytic mechanism of nanosized CdS coupled TiO_2 nanocrystals under visible light irradiation, J. Mol. Catal. A: Chem. 244 (2006) 25–32.
[9] D. Chatterjee, S. Dasgupta, Visible light induced photocatalytic degradation of organic pollutants, J. Photochem. Photobiol., C 6 (2005) 186–205.
[10] I. Nakamura, N. Negishi, S. Kutsuna, T. Ihara, S. Sugihara, K. Takeuchi, Role of oxygen vacancy in the plasma-treated TiO_2 photocatalyst with visible light activity for NO removal, J. Mol. Catal. A: Chem. 161 (2000) 205–212.
[11] S. Rehman, R. Ullah, A.M. Butt, N.D. Gohar, Strategies of making TiO_2 and ZnO visible light active, J. Hazard. Mater. 170 (2009) 560–569.
[12] D. Li, H. Haneda, Synthesis of nitrogen-containing ZnO powders by spray pyrolysis and their visible-light photocatalysis in gas-phase acetaldehyde decomposition, J. Photochem. Photobiol., A 155 (2003) 171–178.
[13] F. Peng, L. Cai, L. Huang, H. Yu, H. Wang, Preparation of nitrogen-doped titanium dioxide with visible-light photocatalytic activity using a facile hydrothermal method, J. Phys. Chem. Solids 69 (2008) 1657–1664.
[14] K. Kobayakawa, Y. Murakami, Y. Sato, Visible-light active N-doped TiO_2 prepared by heating of titanium hydroxide and urea, J. Photochem. Photobiol., A 170 (2005) 177–179.
[15] D. Li, H. Haneda, S. Hishita, N. Ohashi, Visible-light-driven nitrogen-doped TiO_2 photocatalysts: Effect of nitrogen precursors on their photocatalysis for decomposition of gas-phase organic pollutants, Mater. Sci. Eng., B 117 (2005) 67–75.
[16] H. Irie, Y. Watanabe, K. Hashimoto, Nitrogen concentration dependence on photo catalytic activity of $TiO_{2-x}N_x$ powders, J. Phys. Chem. B 107 (2003) 5483–5486.
[17] Z. Wu, F. Dong, W. Zhao, S. Guo, Visible light induced electron transfer process over nitrogen doped TiO_2 nanocrystals prepared by oxidation of titanium nitride, J. Hazard. Mater. 157 (2008) 57–63.
[18] M. Xing, J. Zhang, F. Chen, New approaches to prepare nitrogen doped TiO_2 photocatalysts and study their photo catalytic activities in visible light, Appl. Catal., B 89 (2009) 563–569.
[19] J. Sun, L. Qiao, S. Sun, G. Wang, Photo catalytic degradation of Orange G on nitrogen-doped TiO_2 catalysts under visible light and sunlight irradiation, J. Hazard. Mater. 155 (2008) 312–319.
[20] J.C. Sin, S.M. Lam, K.T. Lee, A.R. Mohamed, Degrading two endocrine-disrupting chemicals from water by UV irradiation with the presence of nanophotocatalysts, Desalin. Water Treat. 51 (2013) 3505–3520.
[21] S.M. Lam, J.C. Sin, A.Z. Abdullah, A.R. Mohamed, Photo catalytic degradation of resorcinol, an endocrine disrupter, by TiO_2 and ZnO suspensions, Environ. Technol. 34 (2013) 1097–1106.
[22] H.M. Santos, C. Loderio, J. Capelo-Martinez, The power of ultrasound, in: J.L. Capelo-Martinez (Ed.), Ultrasound in Chemistry: Analytical Application, Wiley–VCH verlag, Weinheim, 2009, pp. 1–16.
[23] G. Li, J.C. Yu, D. Zhang, X. Hu, W.M. Lau, A mesoporous TiO_2−xNx photocatalyst prepared by sonication pretreatment and *in situ* pyrolysis, Sep. Purif. Technol. 67 (2009) 152–157.
[24] J.A. Cha, S.H. An, H.D. Jang, C.S. Kim, D.K. Song, T.O. Kim, Synthesis and photo catalytic activity of N-doped TiO_2/ ZrO_2 visible-light photocatalysts, Adv. Powder Technol. 23 (2011) 717–723.
[25] Y.Y. Gurkan, N. Turkten, A. Hatipoglu, Z. Cinar, Photo catalytic degradation of cefazolin over N-doped TiO_2 under UV and sunlight irradiation: Prediction of the reaction paths via conceptual DFT, Chem. Eng. J. 184 (2012) 113–124.
[26] Y. Cong, J. Zhang, F. Chen, M. Anpo, Synthesis and characterization of nitrogen-doped TiO_2 nanophotocatalyst with high visible light activity, J. Phys. Chem. C 111 (2007) 6976–6982.
[27] R. Kralchevska, M. Milanova, D. Hristov, A. Pintar, D. Todorovsky, Synthesis, characterization and photocatalytic activity of neodymium, nitrogen and neodymium-nitrogen doped TiO_2, Mater. Res. Bull. 47 (2012) 2165–2177.
[28] B. Kosowska, S. Mozia, A.W. Morawski, B. Grzmil, M. Janus, K. Kałucki, The preparation of TiO_2-nitrogen doped by calcinations of TiO_2.H_2O under ammonia atmosphere for visible light photocatalysis, Sol. Energy Mater. Sol. Cells 88 (2005) 269–280.
[29] H.J. Cho, P.G. Hwang, D. Jung, Preparation and photocatalytic activity of nitrogen-doped TiO2 hollow nanospheres, J. Phys. Chem. Solids 72 (2011) 1462–1466.
[30] X. Cheng, X. Yu, Z. Xing, Characterization and mechanism analysis of N-doped TiO_2 with visible light response and its enhanced visible activity, Appl. Surf. Sci. 258 (2012) 3244–3248.